

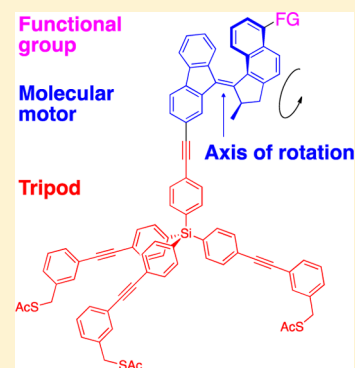
# Control of Surface Wettability Using Tripodal Light-Activated Molecular Motors

Kuang-Yen Chen, Oleksii Ivashenko, Gregory T. Carroll, Jort Robertus, Jos C. M. Kistemaker, Gábor London, Wesley R. Browne, Petra Rudolf, and Ben L. Feringa\*

Centre for Systems Chemistry, Stratingh Institute for Chemistry and Zernike Institute for Advanced Materials, University of Groningen, Nijenborgh 4, 9747 AG, Groningen, The Netherlands

**S** Supporting Information

**ABSTRACT:** Monolayers of fluorinated light-driven molecular motors were synthesized and immobilized on gold films in an altitudinal orientation *via* tripodal stators. In this design the functionalized molecular motors are not interfering and preserve their rotary function on gold. The wettability of the self-assembled monolayers can be modulated by UV irradiation.



## INTRODUCTION

One of the major challenges in nanotechnology is to demonstrate that molecular machines can be harnessed to perform useful work.<sup>1</sup> Inspired by the machines of the macroscopic world, molecular tweezers, propellers, gears, brakes, elevators, valves, rotors, switches, and nanocars have been developed.<sup>2</sup> Additionally, it has been shown that molecular switches and motors can be used to perform various tasks in solution, such as modulation of supramolecular organization,<sup>3</sup> host–guest interactions,<sup>4</sup> controlling the chiral space in which a catalytic reaction takes place,<sup>5</sup> and synthesizing a peptide in a sequence-specific manner.<sup>6</sup>

Confining molecules at an interface inhibits Brownian motion and allows for the modification of the surface properties of a material or even the possibility to perform work at the molecular level through externally induced reversible structural changes.<sup>7</sup> In recent years, increasing attention has focused on surface-immobilized systems containing molecules that are capable of undergoing reversible structural changes upon the application of external stimuli.<sup>8</sup> Various types of external stimuli *i.e.*, chemical,<sup>9</sup> electric,<sup>10</sup> or light<sup>8a</sup> can be applied to address molecules on surfaces. Among these stimuli the use of light, which allows spatial temporal control,<sup>11</sup> is of particular interest due to the potential fast response times of photochemical processes and because light provides a clean, noninvasive, and tunable energy input.<sup>12</sup>

Surfaces functionalized with photoresponsive azobenzene or spirocyclic derivatives have been widely studied due to the propensity for these interfaces to undergo reversible light-induced wettability changes.<sup>13</sup> Azobenzenes exhibit a change in conformation and dipole moment upon  $E \rightarrow Z$  photo-

isomerization, resulting in changes to the polarity and accordingly the wettability of the surface.<sup>14</sup> Spiropyran can also be switched photochemically between a relatively hydrophobic spirocyclic and a hydrophilic merocyanine form which induces a large change in molecular dipole moment.<sup>15</sup> A number of approaches have been developed in order to enhance the wettability contrast between the two states of the azobenzene- and spirocyclic-functionalized surfaces by using mixed layers,<sup>16</sup> increasing surface roughness,<sup>13a</sup> and using polymer-based surfaces.<sup>17</sup> However, controlling the water contact angle (WCA) on flat and smooth surfaces functionalized with photoresponsive organic monolayers remains challenging. The change of the WCA of azobenzene monolayers is typically of the order of 2–14°,<sup>18</sup> and amounts to 5–14°<sup>19</sup> for spirocyclic monolayers. Such modest changes encourage efforts to design and study new responsive surfaces *via* the assembly of photochromic organic monolayers on flat substrates.

Light-driven molecular motors based on overcrowded alkenes<sup>20</sup> are a unique class of organic molecules that are able to use light to power unidirectional rotation. When such molecules are attached to a surface, two types of orientation can be distinguished: azimuthal<sup>21</sup> and altitudinal<sup>22</sup> (Figure 1). Motors rotating in an altitudinal orientation relative to the surface are expected to have great potential for the construction of photoswitchable surfaces because the exposure of a functional group on the rotor can be modulated in a cyclic fashion.<sup>22d</sup> Despite the promise of altitudinal motors in

Received: December 3, 2013

Published: February 3, 2014

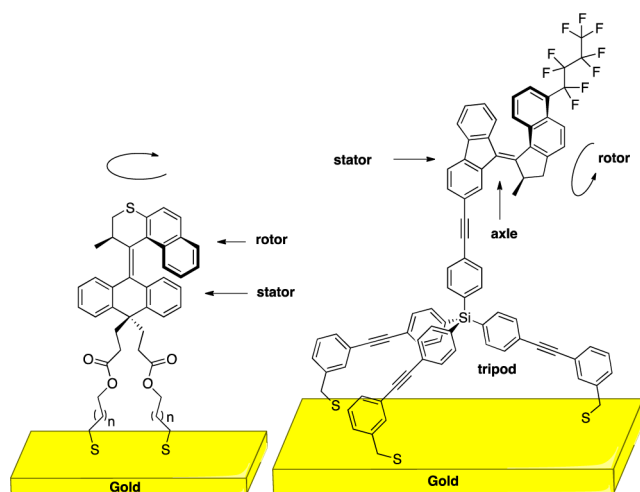


**Figure 1.** Azimuthal (left) and altitudinal (right) molecular motors on surfaces.

powering surface-mounted nanomachinery, the speed of rotation has been shown to be affected by intermolecular interactions.<sup>22b</sup> Although dilution (mixed monolayers) can minimize molecular interactions (but with the consequence of fewer molecular motors on the surface), the anticipated dynamic change in properties of these systems is reduced. A key challenge in developing surface-bound devices based on molecular motors is to exploit the collective motion of the motor to interact with an external species in a dynamic manner. One way to demonstrate that the rotary motion of a surface-bound layer of oriented motors can collectively influence interactions with an overlayer material is to monitor the contact angle of a liquid on top of the motor monolayer. Changes in the contact angle of a liquid droplet at the surface of the motor layer can be correlated to collective changes in the orientation of the rotor moieties with respect to the surface. Disruptive interactions between motors are expected to be minimized by designing motors with bulky stators that minimize the interaction between the rotor parts.

To date, light-driven, rotary, molecular-motor-based surfaces that undergo changes in wettability upon irradiation have not been reported. The wettability of a recently reported surface containing a monolayer of altitudinal motors was shown to depend on whether the motors were assembled in the *cis* or *trans* form.<sup>22d</sup> However, once the motors were assembled, the wettability could not be modified, which was attributed to a lower photoconversion when motors are confined to a crowded monolayer compared to when in solution.

Herein we report a novel altitudinal light-driven molecular motor design comprising a rotor with a hydrophobic perfluorobutyl group and a tripodal stator containing thiol groups for self-assembly on gold (Figure 1, right). The bulky stator increases the spacing between the rotors of the surface-bound motors sufficiently to facilitate unobstructed rotary motion. Water droplets placed on the motor-modified surfaces undergo changes in the contact angle upon irradiation of the surfaces with UV light. This is the first example showing that the wetting properties of surfaces functionalized with molecular motors based on overcrowded alkenes can be modulated with light.

## RESULTS AND DISCUSSION

**Design of the Photoresponsive Molecular Motor.** The parent motor **8** (Scheme 1) was selected, as it exhibits a substantial barrier toward thermal isomerization,<sup>23</sup> making this step slow at room temperature and thus facilitating characterization of the separate states during the rotary cycle in solution and on the surface. In addition, a hydrophobic perfluorobutyl group was incorporated onto the rotor part of the altitudinal motor in order to enhance the surface wettability changes upon switching.

A tripod<sup>24</sup> was chosen as the surface anchoring group for the following reasons: (1) The rigid tripod is a promising stator to anchor the motor in a fixed and altitudinal orientation with respect to the surface; (2) as we reported previously, when the motor-embedded chromophores are assembled too close to the gold substrate (Figure 1, left,  $n = 1$ ), energy transfer from the excited state of the motor to the gold substrate may occur,<sup>21a</sup> preventing the motor from rotating. Mounting the motor onto tripodal legs allows binding to gold in a rigid manner that is expected to sufficiently isolate the motor from the surface, allowing efficient photoinduced isomerization (Figure 1); (3) it was previously shown that the attachment of overcrowded alkenes to surfaces *via* two-legs results in a high density of packing.<sup>22b</sup> The increase of the half-life of the thermal isomerization step indicates intermolecular interactions between the surface-bound overcrowded alkenes, resulting in a decrease in the overall speed of the rotary cycle.<sup>22b,25</sup>

The bulky tripodal structure presented in this report is an ideal candidate to create free volume between the rotors, limiting interactions between the surface-bound motors and also enforcing altitudinal orientation. Calculations show that the area occupied by the tripod is expected to exceed the theoretical dimensions of the motor unit (Figure 1 and Figure S10, see Supporting Information [SI]).

**Synthesis.** The approach toward the synthesis of motor **1**, which bears a perfluorobutyl chain at the rotor and a tripod at the stator to allow surface attachment, is depicted in Scheme 1.

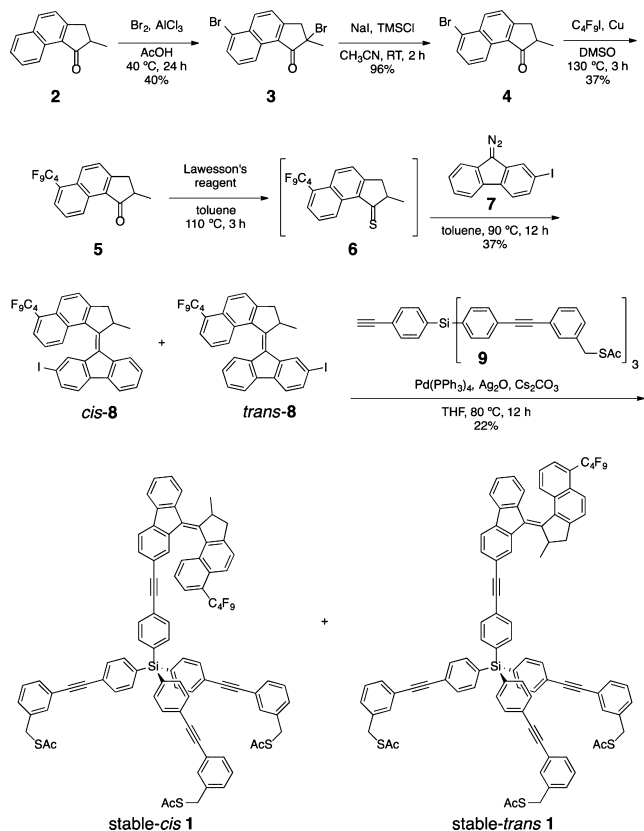
Starting from **2**, which was synthesized by a one pot Friedel–Crafts acylation/Nazarov cyclization, ketone **2** was subsequently brominated by treating it with 4 equiv of bromine in the presence of  $\text{AlCl}_3$  in  $\text{AcOH}$  to form dibromosubstituted **3**. The  $\alpha$ -bromo substituent in **3** was removed by treatment with  $\text{NaI}$  and  $\text{TMSCl}$  in  $\text{CH}_3\text{CN}$  to form **4**. The perfluorobutyl chain was introduced by treating **4** with nonafluoro-1-iodobutane and copper/bronze in  $\text{DMSO}$ , affording **5**.

Ketone **5** was treated with Lawesson's reagent in toluene to give the reactive thioketone **6**. The key step in the synthesis of **8**, which has a highly sterically hindered double bond, is the Barton–Kelllogg diazo–thioketone coupling.<sup>26</sup> This coupling was performed by heating thioketone **6** and diazo compound **7** in toluene at reflux to afford overcrowded alkene **8** as a mixture of *cis* and *trans* isomers.

Motor **8** and tripod **9** were connected by a Sonogashira<sup>27</sup> coupling reaction in the presence of  $\text{Pd}(\text{PPh}_3)_4$ , providing **1** in 22% yield as a mixture of *cis* and *trans* isomers. Preparative thin layer chromatography provided pure stable-*cis* **1** and stable-*trans* **1**. Their configuration was assigned by comparison of their  $^1\text{H}$  NMR spectra with those of previously reported structurally related motors.<sup>28</sup>

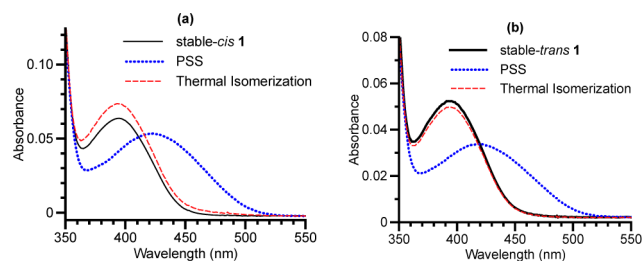
**Photochemical and Thermal Behavior of Molecular Motor **1** in Solution.** Photochemical and thermal isomerization studies were carried out in solution using both low-

## Scheme 1. Synthesis of Molecular Motor 1



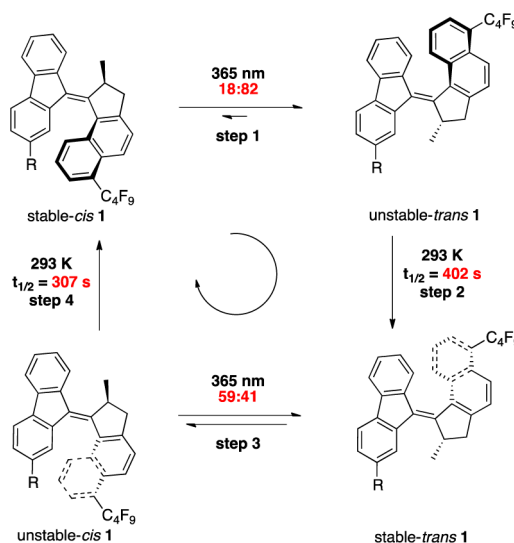
temperature UV/vis absorption and  $^1\text{H}$  NMR spectroscopy to demonstrate that stable-*cis* **1** and stable-*trans* **1** operate as molecular motors.<sup>20</sup>

The UV/vis absorption spectra of stable-*cis* **1** ( $4.07 \times 10^{-6}$  M) and stable-*trans* **1** ( $2.73 \times 10^{-6}$  M) in  $\text{CH}_2\text{Cl}_2$  at 253 K both show absorption bands centered at 395 nm (Figure 2, solid lines).



**Figure 2.** UV/vis absorption spectra ( $\text{CH}_2\text{Cl}_2$ , 253 K) of stable-*cis* **1** (a) and stable-*trans* **1** (b) (solid line). The spectra after UV irradiation (photoisomerization) (dotted line) and heating (thermal isomerization) (dashed line) are also shown.

Irradiation of the same sample with UV light ( $\lambda_{\text{max}} = 365$  nm) resulted in a red-shift of the band at 395 nm to an absorption centered at 450 nm, indicating the photochemically induced formation of the unstable isomers (Figure 2, dotted lines; Scheme 2, step 1 or 3). This red-shift is consistent with increased strain at the central double bond, and hence the generation of a higher-energy isomer.<sup>29</sup> During the irradiation of each compound, clear isosbestic points were maintained, indicating that the photoisomerization was a unimolecular process.

Scheme 2. Full 360° Rotary Cycle for Molecular Motor **1** ( $R = 9$ , Scheme 1)

Samples were irradiated until no further changes were observed, indicating that the photostationary state (PSS) was reached (Figure 2, dotted lines). Allowing the solutions to warm to room temperature resulted in a blue-shift of the band at 450 to 395 nm, which is consistent with thermal isomerization to the corresponding stable isomers (Figure 2, dashed lines; Scheme 2, step 2 or 4).

Kinetic analysis was performed on both thermal isomerization steps (Scheme 2, steps 2 and 4; Figure S2, see the SI). For unstable-*trans* **1**  $\rightarrow$  stable-*trans* **1**, the Gibbs free energy of activation ( $\Delta^\ddagger G^\circ$ ) was 87.29 kJ/mol ( $t_{1/2} = 402$  s at RT) and for unstable-*cis* **1**  $\rightarrow$  stable-*cis* **1**,  $\Delta^\ddagger G^\circ = 87.41$  kJ/mol ( $t_{1/2} = 307$  s at RT). These values are similar to those obtained from structurally related motors.<sup>28</sup>

The photostationary states, 18/82 for stable-*cis* **1**/unstable-*trans* **1** and 49/59 for stable-*trans* **1**/unstable-*cis* **1**, were determined by low temperature  $^1\text{H}$  NMR spectroscopy (Figure S3 and S4, see SI).

By studying the photochemical and thermal behavior of **1** in solution using a combination of UV/vis and  $^1\text{H}$  NMR spectroscopy, and by analogy with similar motor systems reported previously,<sup>28</sup> it is concluded that **1** functions as a light-driven rotary motor in solution.

In summary, the introduction of the tripod and a perfluorobutyl group on the motor moiety does not have a significant influence on the photochemical and thermal behavior of the motor.

**Surface Attachment and Characterization.** Immobilization of motor **1** on surfaces was achieved by immersion of a gold substrate in a solution of stable-*cis* **1** or stable-*trans* **1** with hydrazine as a deprotecting reagent. (Scheme 3, for further details on surface preparations, see the SI) The mean monolayer thickness values of  $16.9 \pm 0.3$  Å for stable-*cis* **1** SAM and  $18.4 \pm 0.1$  Å for stable-*trans* **1** SAM were determined by XPS<sup>30</sup> and are in good agreement with similar overcrowded alkene systems assembled on a variety of surfaces previously reported by our group.<sup>22a,25,31</sup> The surface coverage on gold ( $2.2 \times 10^{-11}$  mol  $\text{cm}^{-2}$  for stable-*cis* **1** SAM and  $2.4 \times 10^{-11}$  mol  $\text{cm}^{-2}$  for stable-*trans* **1** SAM, determined by UV/vis spectroscopy, Figures 2 and 3) are consistent with single-layer formation.

## Scheme 3. Immobilization of Molecular Motor 1 onto a Gold Film

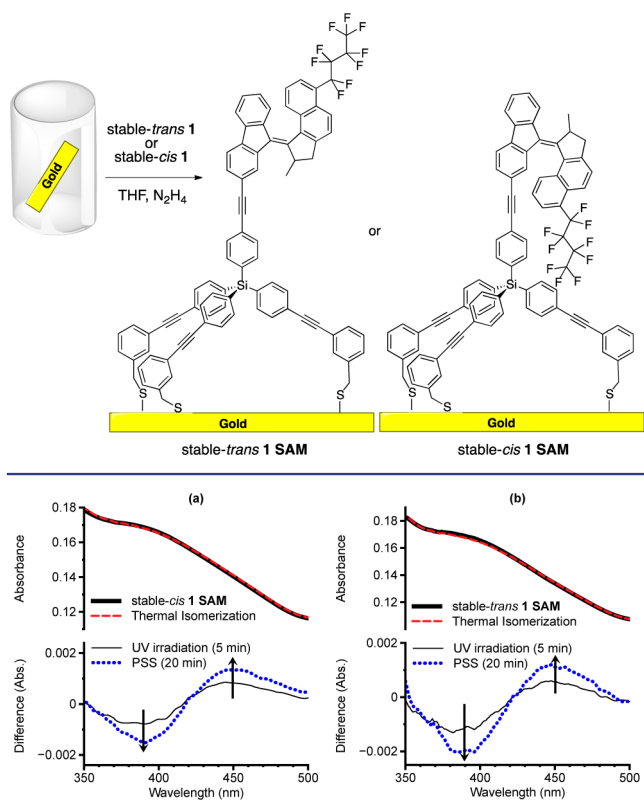


**Figure 3.** UV/vis absorption spectra of (a) stable-*cis* 1 SAM and (b) stable-*trans* 1 SAM (solid thick lines). Both isomers undergo photoisomerization upon UV irradiation, and the difference between the spectra of the initial state and irradiated samples are shown (thin solid and dotted lines at lower panel). The spectra after thermal isomerization are also shown (dashed lines). For discussion of response time, see also SI S12.

The UV/vis absorption spectra of stable-*cis* and stable-*trans* 1 SAMs showed the characteristic absorption of the motors after rinsing the substrates copiously with THF and methanol, indicating that the attachment of motor 1 on the gold substrate was successful. (Figure 3, solid line). The major absorption bands (centered at 395 nm for stable 1 SAMs) are similar to those observed for 1 in CH<sub>2</sub>Cl<sub>2</sub> solution (Figure 2).

Irradiation of stable 1 SAMs with UV light ( $\lambda_{\max} = 365$  nm) resulted in a red-shift in the UV/vis absorption to 450 nm (Figure 3, lower panel) similar to that observed in CH<sub>2</sub>Cl<sub>2</sub> solution (Figure 2), indicating the formation of the unstable form of the surface-bound motors (Scheme 2, steps 1 and 3). After keeping the surfaces in the dark at room temperature for 12 h, the original UV/vis absorption spectra recovered, which is consistent with the thermal isomerization of the motors. (Figure 3, dashed line; Scheme 2, step 2 or 4)

In order to compare the surface-bound system with the solution analogue, we followed the thermal isomerization by monitoring the change in the UV/vis spectra at 450 nm as a function of time. (Figure S6, see SI) The thermal decay of the signals were fitted with monoexponential decay, and the half-life for unstable-*cis* 1 SAM  $\rightarrow$  stable-*cis* 1 SAM ( $t_{1/2} = 351$  s at RT) and unstable-*trans* 1 SAM  $\rightarrow$  stable-*trans* 1 SAM ( $t_{1/2} = 530$  s at RT) were extracted. These values are similar to those observed in CH<sub>2</sub>Cl<sub>2</sub> solution (Scheme 2) showing that the

thermal isomerization steps were not inhibited using the tripod as a surface attachment group and spacer between the motor and gold film. The bulky structure of the tripod increases the distance between motor chromophores in the surface-bound monolayer, minimizing inter-rotor interactions.

The overview X-ray photoelectron (XPS) scans of the monolayers stable-*cis* 1 SAM and stable-*trans* 1 SAM before and after UV irradiation for 2 h are also shown (Figure S8, see SI). The spectra obtained after UV irradiation qualitatively resemble those collected on the pristine 1 SAMs, indicating the stability of the motor and tripod moieties on the gold surface under exposure to UV light for a considerable amount of time.

Water contact angle (WCA) measurements were performed on motor 1 SAM on flat gold (150 nm Au/mica) in order to determine the wettability of the monolayers. In the case of stable-*cis* 1 SAM, where the hydrophobic perfluorobutyl group is likely to be hidden from the interface, a contact angle of  $60 \pm 1^\circ$  was measured; however, stable-*trans* 1 SAM, where the perfluorobutyl groups are exposed to the interface, shows a contact angle of  $82 \pm 1^\circ$  (Figure 4), which is attributed to the hydrophobic nature of the perfluorobutyl chain.

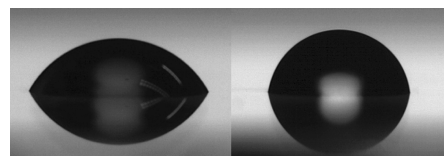


**Figure 4.** Water droplet on stable-*cis* 1 SAM (left) and stable-*trans* 1 SAM (right).

In the present system using an altitudinal molecular motor, control of surface wettability was achieved by irradiating both 1 SAMs with UV light ( $\lambda_{\max} = 365$  nm), which resulted in WCA changes of the stable-*cis* 1 SAM from  $60 \pm 1^\circ$  to  $76 \pm 1^\circ$  and for the stable-*trans* 1 SAM,  $82 \pm 1^\circ$  to  $68 \pm 1^\circ$ . (Table 1). The changes in WCA after UV irradiation are a manifestation of the photoinduced switching of the motors on gold and are consistent with UV/vis spectroscopic data (Figure 3).

**Table 1.** Water Contact Angle for Stable-*cis* 1 SAM and Stable-*trans* 1 SAM before and after UV Irradiation on Flat Surface

	contact angle (deg)	
	before irradiation	after irradiation
stable- <i>cis</i> 1 SAM	$60 \pm 1$	$76 \pm 1$
stable- <i>trans</i> 1 SAM	$82 \pm 1$	$68 \pm 1$

The ratios between stable-*cis* 1 and unstable-*trans* 1 or stable-*trans* 1 and unstable-*cis* 1 are 18:82 or 41:59 in solution, respectively, at the photostationary state (PSS<sub>365 nm</sub>, Scheme 2). The separation between the molecular motors and the surface as well as each other achieved with the present immobilization approach means that it would be reasonable to expect that the PSS achieved in solution is retained in the SAMs also. Indeed, on the first cycle the changes observed are consistent with the PSS observed in solution. Hence, upon irradiation of the molecular motors anchored on the surface, the changes in wettability are not expected to show full reversibility over several cycles but instead reach an intermediate situation between purely *cis*- and *trans*- states, as is observed

experimentally (Figure S9, see SI; For switching efficiency, see also S13 in SI). These data demonstrate that the design employed in anchoring the molecular motor to the surface allows light to be used to change molecular state and thereby achieve the highly challenging task of changing wettability with an external stimulus.

Modifying the wettability of a substrate with a monolayer of rotary motors upon irradiation is unprecedented. Previously, surfaces functionalized with *cis* or *trans* isomers of altitudinal motors with the same perfluorobutyl chain on the rotor as reported here showed only a difference of 12° in WCA between the *cis* and *trans* surfaces, and the surface wettability could not be modified by UV irradiation.<sup>22d</sup> Presumably, without the bulky tripod spacer the motor chromophores are too crowded to allow for a sufficient yield of photoisomerization to detect an appreciable change in macroscopic properties.<sup>22d</sup>

Incorporating three phenyl-acetylene-based “legs” into the structure of the motor increases the space between the rotors, allowing for facile rotary motion and hence modification of the surface properties.

## CONCLUSIONS

Motors bearing a hydrophobic perfluorobutyl group on the rotor and a rigid phenyl-acetylene-based tripod on the stator were successfully synthesized and attached to a gold surface.

The spacing between the motor and the gold surface is sufficient to effectively compete with quenching of the excited state by the gold surface and to allow for photoisomerization of the central alkene. Confinement of altitudinal motors at surfaces *via* flexible long chains was reported to reduce the rate of the thermal isomerization process,<sup>22b</sup> however, the system described herein has overcome this issue. In the present system the thermal isomerization is not inhibited, showing that the tripod is an ideal surface anchoring group to prevent the motors from interacting with each other and from interacting directly with the underlying gold substrate.

Additionally, although previously reported nonsymmetric altitudinal motors bearing fluoro groups were unable to change the water contact angle by irradiation post-assembly, the current system can change the contact angle of a water drop by up to 16° upon irradiation of the motor–water interface. This is the first example of controlling the surface wettability of a monolayer of motors by irradiation. The tripod structure minimizes obstruction of the rotary cycle and enhances the ability to modulate collective interactions at the motor–water interface. The current design features will be key to fabricating future nanoscale systems that can be used to exploit the rotary cycle to perform work at the molecular level, to control interactions with surface adsorbates and to apply single-molecule techniques to measure the rotation of a single motor on a surface.

## ASSOCIATED CONTENT

### Supporting Information

Synthesis and characterization of new compounds, Eyring plots for the kinetic studies of motor **1**, <sup>1</sup>H spectra after photochemical and thermal isomerization for **1**, the procedures for preparing the monolayers, XPS spectra of the **1** SAMs, theoretical calculation of **1**. This material is available free of charge via the Internet at <http://pubs.acs.org>.

## AUTHOR INFORMATION

### Corresponding Author

B.L.Feringa@rug.nl

### Notes

The authors declare no competing financial interest.

## ACKNOWLEDGMENTS

Financial support from NanoNed, The Netherlands Organization for Scientific Research (NWO-CW); the European Research Council (Advanced Investigator Grant, No. 227897 to B.L.F.); funding from the Ministry of Education, Culture and Science (Gravity program 024.001.035); and the “Top Research School” program of the Zernike Institute for Advanced Materials under the Bonus Incentive Scheme (BIS) are gratefully acknowledged.

## REFERENCES

- (1) (a) Saha, S.; Stoddart, J. F. *Chem. Soc. Rev.* **2006**, *36*, 77–92. (b) Browne, W. R.; Feringa, B. L. *Nat. Nanotechnol.* **2006**, *1*, 25–35. (c) Kay, E. R.; Leigh, D. A.; Zerbetto, F. *Angew. Chem., Int. Ed.* **2007**, *46*, 72–191. (d) *Molecular Devices and Machines: Concepts and Perspectives for the Nanoworld*; Balzani, V., Credi, A., Venturi, M., Eds.; Wiley-VCH: Weinheim, 2008. (e) *Non-Covalent Assemblies to Molecular Machines*; Sauvage, J.-P., Gaspard, P., Eds.; Wiley-VCH: Weinheim, 2010. (f) Coskun, A.; Banaszak, M.; Astumian, R. D.; Stoddart, J. F.; Grzybowski, B. A. *Chem. Soc. Rev.* **2012**, *41*, 19–30.
- (2) (a) Kinbara, K.; Aida, T. *Chem. Rev.* **2005**, *105*, 1377–1400. (b) Kottas, G. S.; Clarke, L. I.; Horinek, D.; Michl, J. *Chem. Rev.* **2005**, *105*, 1281–1376. (c) Michl, J.; Sykes, E. C. H. *ACS Nano* **2009**, *3*, 1042–1048. (d) Kudernac, T.; Ruangsapapichat, N.; Parschau, M.; Maciá, B.; Katsonis, N.; Harutyunyan, S. R.; Ernst, K.-H.; Feringa, B. L. *Nature* **2011**, *479*, 208–211. (e) *Molecular Switches*; Browne, W. R., Feringa, B. L., Eds.; Wiley-VCH: Weinheim, 2011. (f) Szymański, W.; Beierle, J. M.; Kistemaker, H. A. V.; Velema, W. A.; Feringa, B. L. *Chem. Rev.* **2013**, *113*, 6114–6178.
- (3) de Jong, J. J.; Lucas, L. N.; Kellogg, R. M.; Van Esch, J. H.; Feringa, B. L. *Science* **2004**, *304*, 278–281.
- (4) Thomas, C. R.; Ferris, D. P.; Lee, J.-H.; Choi, E.; Cho, M. H.; Kim, E. S.; Stoddart, J. F.; Shin, J.-S.; Cheon, J.; Zink, J. I. *J. Am. Chem. Soc.* **2010**, *132*, 10623–10625.
- (5) Wang, J.; Feringa, B. L. *Science* **2011**, *331*, 1429–1432.
- (6) Lewandowski, B.; De Bo, G.; Ward, J. W.; Pappmeyer, M.; Kuschel, S.; Aldegunde, M. J.; Gramlich, P. M. E.; Heckmann, D.; Goldup, S. M.; D’Souza, D. M.; Fernandes, A. E.; Leigh, D. A. *Science* **2013**, *339*, 189–193.
- (7) (a) Hugel, T.; Holland, N. B.; Cattani, A.; Moroder, L.; Seitz, M.; Gaub, H. E. *Science* **2002**, *296*, 1103–1106. (b) Liu, Y.; Flood, A. H.; Bonvallet, P. A.; Vignon, S. A.; Northrop, B. H.; Tseng, H.-R.; Jeppesen, J. O.; Huang, T. J.; Brough, B.; Baller, M.; Magonov, S.; Solares, S. D.; Goddard, W. A.; Ho, C.-M.; Stoddart, J. F. *J. Am. Chem. Soc.* **2005**, *127*, 9745–9759. (c) Ferri, V.; Elbing, M.; Pace, G.; Dickey, M. D.; Zharnikov, M.; Samori, P.; Mayor, M.; Rampi, M. A. *Angew. Chem., Int. Ed.* **2008**, *47*, 3407–3409. (d) Robertus, J.; Browne, W. R.; Feringa, B. L. *Chem. Soc. Rev.* **2010**, *39*, 354–378. (e) Nakanishi, H.; Bishop, K. J. M.; Kowalczyk, B.; Nitzan, A.; Weiss, E. A.; Tretiakov, K. V.; Apodaca, M. M.; Klajn, R.; Stoddart, J. F.; Grzybowski, B. A. *Nature* **2009**, *460*, 371–375.
- (8) (a) Katsonis, N.; Lubomska, M.; Pollard, M. M.; Feringa, B. L.; Rudolf, P. *Prog. Surf. Sci.* **2007**, *82*, 407–434. (b) Browne, W. R.; Feringa, B. L. *Annu. Rev. Phys. Chem.* **2009**, *60*, 407–428.
- (9) Ye, T.; Kumar, A. S.; Saha, S.; Takami, T.; Huang, T. J.; Stoddart, J. F.; Weiss, P. S. *ACS Nano* **2010**, *4*, 3697–3701.
- (10) Alemani, M.; Peters, M. V.; Hecht, S.; Rieder, K.-H.; Moresco, F.; Grill, L. *J. Am. Chem. Soc.* **2006**, *128*, 14446–14447.
- (11) Velema, W. A.; van der Berg, J. P.; Hansen, M. J.; Szymański, W.; Driessen, A. J. M.; Feringa, B. L. *Nat. Chem.* **2013**, *5*, 924–928.

- (12) Zheng, Y. B.; Pathem, B. K.; Hohman, J. N.; Thomas, J. C.; Kim, M.; Weiss, P. S. *Adv. Mater.* **2013**, *25*, 302–312.
- (13) (a) Ichimura, K.; Oh, S. K.; Nakagawa, M. *Science* **2000**, *288*, 1624–1626. (b) Berná, J.; Leigh, D. A.; Lubomska, M.; Mendoza, S. M.; Pérez, E. M.; Rudolf, P.; Teobaldi, G.; Zerbetto, F. *Nat. Mater.* **2005**, *4*, 704–710. (c) Yang, D.; Piech, M.; Bell, N. S.; Gust, D.; Vail, S.; Garcia, A. A.; Schneider, J.; Park, C.-D.; Hayes, M. A.; Picraux, S. T. *Langmuir* **2007**, *23*, 10864–10872. (d) Xin, B.; Hao, J. *Chem. Soc. Rev.* **2010**, *39*, 769–782.
- (14) Klajn, R. *Pure Appl. Chem.* **2010**, *82*, 2247–2279.
- (15) Berkovic, G.; Krongauz, V.; Weiss, V. *Chem. Rev.* **2000**, *100*, 1741–1754.
- (16) Lim, H. S.; Han, J. T.; Kwak, D.; Jin, M.; Cho, K. *J. Am. Chem. Soc.* **2006**, *128*, 14458–14459.
- (17) (a) Feng, C. L.; Zhang, Y. J.; Jin, J.; Song, Y. L.; Xie, L. Y.; Qu, G. R.; Jiang, L.; Zhu, D. B. *Langmuir* **2001**, *17*, 4593–4597. (b) Groten, J.; Bunte, C.; Rühle, J. *Langmuir* **2012**, *28*, 15038–15046.
- (18) (a) Siewierski, L. M.; Brittain, W. J.; Petrash, S.; Foster, M. D. *Langmuir* **1996**, *12*, 5838–5844. (b) Oh, S.-K.; Nakagawa, M.; Ichimura, K. *J. Mater. Chem.* **2002**, *12*, 2262–2269. (c) Hamelmann, F.; Heinzmann, U.; Siemeling, U.; Bretthauer, F.; Vor der Brüggen, J. *Appl. Surf. Sci.* **2004**, *222*, 1–5. (d) Delorme, N.; Bardeau, J. F.; Bulou, A.; Poncin-Epaillard, F. *Langmuir* **2005**, *21*, 12278–12282.
- (19) (a) Rosario, R.; Gust, D.; Hayes, M.; Jahnke, F.; Springer, J.; Garcia, A. A. *Langmuir* **2002**, *18*, 8062–8069. (b) Rosario, R.; Gust, D.; Garcia, A. A.; Hayes, M.; Taraci, J. L.; Clement, T.; Dailey, J. W.; Picraux, S. T. *J. Phys. Chem. B* **2004**, *108*, 12640–12642. (c) Dattilo, D.; Armelao, L.; Fois, G.; Mistura, G.; Maggini, M. *Langmuir* **2007**, *23*, 12945–12950.
- (20) (a) Koumura, N.; Zijlstra, R. W.; van Delden, R. A.; Harada, N.; Feringa, B. L. *Nature* **1999**, *401*, 152–155. (b) *Molecular Motors*; Schliwa, M., Ed.; Wiley-VCH: Weinheim, 2003.
- (21) (a) Carroll, G. T.; Pollard, M. M.; van Delden, R.; Feringa, B. L. *Chem. Sci.* **2010**, *1*, 97–101. (b) Perera, U. G. E.; Ample, F.; Kersell, H.; Zhang, Y.; Vives, G.; Echeverria, J.; Grisolia, M.; Rapenne, G.; Joachim, C.; Hla, S.-W. *Nat. Nanotechnol.* **2012**, *8*, 46–51.
- (22) (a) London, G.; Carroll, G. T.; Fernández Landaluce, T.; Pollard, M. M.; Rudolf, P.; Feringa, B. L. *Chem. Commun.* **2009**, 1712–1714. (b) Carroll, G. T.; London, G.; Landaluce, T. F.; Rudolf, P.; Feringa, B. L. *ACS Nano* **2011**, *5*, 622–630. (c) London, G.; Carroll, G. T.; Feringa, B. L. *Org. Biomol. Chem.* **2013**, *11*, 3477–3483. (d) London, G.; Chen, K.-Y.; Carroll, G. T.; Feringa, B. L. *Chem.—Eur. J.* **2013**, *19*, 10690–10697.
- (23) Pollard, M. M.; von Wesenhagen, P.; Pijper, D.; Feringa, B. L. *Org. Biomol. Chem.* **2008**, *6*, 1605–1612.
- (24) (a) Shirai, Y.; Cheng, L.; Chen, B.; Tour, J. M. *J. Am. Chem. Soc.* **2006**, *128*, 13479–13489. (b) Shirai, Y.; Guerrero, J. M.; Sasaki, T.; He, T.; Ding, H.; Vives, G.; Yu, B.-C.; Cheng, L.; Flatt, A. K.; Taylor, P. G.; Gao, Y.; Tour, J. M. *J. Org. Chem.* **2009**, *74*, 7885–7897. (c) Wagner, S.; Leyssner, F.; Kördel, C.; Zarwell, S.; Schmidt, R.; Weinelt, M.; Rück-Braun, K.; Wolf, M.; Tegeder, P. *Phys. Chem. Chem. Phys.* **2009**, *11*, 6242–6248.
- (25) Ivashenko, O.; Logtenberg, H.; Areephong, J.; Coleman, A. C.; Wesenhagen, P. V.; Geertsema, E. M.; Heuvel, N.; Feringa, B. L.; Rudolf, P.; Browne, W. R. *J. Phys. Chem. C* **2011**, *115*, 22965–22975.
- (26) Buter, J.; Wassenaar, S.; Kellogg, R. M. *J. Org. Chem.* **1972**, *37*, 4045–4060.
- (27) Mori, A.; Kawashima, J.; Shimada, T.; Suguro, M.; Hirabayashi, K.; Nishihara, Y. *Org. Lett.* **2000**, *2*, 2935–2937.
- (28) (a) Vicario, J.; Walko, M.; Meetsma, A.; Feringa, B. L. *J. Am. Chem. Soc.* **2006**, *128*, 5127–5135. (b) Pijper, D.; Feringa, B. L. *Angew. Chem., Int. Ed.* **2007**, *46*, 3693–3696.
- (29) ter Wiel, M. K. J.; van Delden, R. A.; Meetsma, A.; Feringa, B. L. *J. Am. Chem. Soc.* **2005**, *127*, 14208–14222.
- (30) (a) The thickness of the monolayers were calculated from attenuation of the Au 4f signals using XPS, see the Supporting Information (b) Bain, C. D.; Whitesides, G. M. *J. Phys. Chem.* **1989**, *93*, 1670–1673.
- (31) (a) van Delden, R. A.; ter Wiel, M. K. J.; Pollard, M. M.; Vicario, J.; Koumura, N.; Feringa, B. L. *Nature* **2005**, *437*, 1337–1340. (b) Coleman, A. C.; Areephong, J.; Vicario, J.; Meetsma, A.; Browne, W. R.; Feringa, B. L. *Angew. Chem., Int. Ed.* **2010**, *49*, 6580–6584.